JOURNAL OF CATALYSIS 89, 79–92 (1984)

Spectroscopic Study of the Interconversion of Chemisorbed Surface Species: The Reaction $Rh^I(CO)_2 + CO \rightarrow Rh^I(CO)_3$

H. P. WANG AND JOHN T. YATES, JR.

Surface Science Center, Department of Chemistry, University of Pittsburgh, Pittsburgh, Pennsylvania 15260

Received August 1, 1983; revised March 14, 1984

The adsorption of CO onto Rh^I sites produced by O_2 treatment of Rh crystallites supported on Al_2O_3, has been studied using high-sensitivity ir difference spectroscopy. The $Rh^I(CO)_2$ (*gem*-dicarbonyl) species is found to form by means of an activated process, in agreement with previous investigations on unoxidized Rh/Al_2O_3 surfaces. A thorough study of the infrared spectrum of the *gem*-dicarbonyl species as a function of surface concentration indicates that there is only one kind of Rh^I site involved, and that the sharp ir bands observed for $Rh^I(CO)_2$ are homogeneously broadened. We have observed the reversible interconversion process $Rh^I(CO)_2 + CO(g) \rightarrow Rh^I(CO)_3$, and have measured the ir spectrum of the $Rh^I(CO)_3$ species. The presence of three carbonyl stretching modes [2120, 2078, and 2026 cm^{-1}] suggests that the symmetry of the species is below C_{3v}, due to multicoordinated bonding of the Rh^I site to the Al_2O_3 support. The labile $Rh^I(CO)_3$ species is thought to be the surface intermediate responsible for facile isotopic exchange of labeled CO into the *gem*-dicarbonyl species.

I. INTRODUCTION

The characterization of highly dispersed metal catalysts remains a major objective in surface chemistry and in heterogeneous catalysis. It is well known that as metal dispersion is increased, new patterns of catalytic activity and selectivity often result. In the limit of very high metallic dispersion, questions about the structural and electronic character of the metal sites are often raised. The system Rh/Al_2O_3 exhibits unusual adsorption properties toward CO at high Rh dispersion, and there is much evidence that Rh^I sites exist on the Al_2O_3 surface, along with metallic Rh sites. This paper, in a continuation of earlier studies, is focused on the infrared spectroscopic characterization of dicarbonyl and tricarbonyl complexes on these Rh^I sites.

An alternate view of the Rh site responsible for the formation of the dicarbonyl has been given by Yates *et al.* (*1*). They have interpreted this species as being a $Rh^0(CO)_2$ species, where the Rh^0 sites exist at the edges of "rafts" of Rh on the Al_2O_3 surface. This assignment has been supported by Katzer *et al.* (*2*), but there is much opinion in favor of $Rh^I(CO)_2$ (*3–15*). Particularly strong evidence for Rh^I comes from the work of Bilhou (*5*) who showed that the intensity of the *gem*-dicarbonyl infrared spectrum increases after oxidation. Conesa (*8*) also showed that the 373 K reduction of Rh^{III} on TiO_2 by CO to give $Rh^I(CO)_2$ was accompanied by stoichiometric production of CO_2.

The first infrared study of CO chemisorbed on rhodium supported on high-area Al_2O_3 was reported by Yang and Garland (*16*). They provided convincing evidence for a species of the form $Rh^I(CO)_2$ (C_{2v}), the *gem*-dicarbonyl, whose infrared spectrum showed a doublet at $\nu = 2095$ and 2027 cm^{-1} due to symmetric and asymmetric coupling between the two CO ligands. More recent investigations (*11, 12, 17–26*) agree extremely well experimentally with this early work. Recently this *gem*-dicarbonyl species has been assigned to isolated Rh^I sites (*3–15, 22, 23, 25–27*) which coexist on Al_2O_3 with Rh_x^0 cluster or crystallite sites. It has been found that oxidation of supported Rh followed by CO adsorption leads to Rh^I

0021-9517/84 $3.00

$(CO)_2$ as the sole surface species (*12*). Additional observations supporting the vibrational frequency assignment of $Rh^I(CO)_2$ have recently been made by Yates and Kolasinski (*27*). The expected number of isotopic *gem*-dicarbonyl species is observed by infrared spectroscopy, confirming that the surface species is a nonlinear $Rh^I(CO)_2$.

Yates and co-workers have studied the isotopic exchange of $^{13}CO(g)$ with $Rh^I(CO)_2$ finding that the exchange will occur at 200 K at rates which are rapid compared to desorption at this temperature (*11, 17*). Similar results have been observed for the isotopic exchange process of ^{13}CO with chemisorbed ^{12}CO on a Ni(100) single crystal. The isotopic exchange process is very rapid at low temperature ($T \simeq 150$ K) compared to thermal desorption at this temperature (*28*). In order to explain these fast thermal exchange processes, a model has been proposed in which the adsorption site is coordinated to multiple-CO ligands at high CO pressure on both the Ni(100) surface and the supported Rh (*11*). Presumably, the rapid isotopic exchange may occur at high CO pressures via the formation of additional weakly bound ligands which are involved in an associative exchange process. For supported Rh, a reaction such as $Rh^I(CO)_2 + CO(g) \rightarrow Rh^I(CO)_3$ has been postulated (*11*) to explain the preferential rapid exchange of the *gem*-dicarbonyl species compared to CO chemisorbed on Rh_x^0 sites. If the associative mechanism involving the complex $Rh^I(CO)_3$ is operative, one might expect to spectroscopically observe the $Rh^I(CO)_3$ species at low temperatures and high CO pressure, and this objective has been achieved in the work reported here.

Infrared spectroscopy has been shown to be very useful in determining the structure of the adsorbed species on supported metal surfaces (*29, 30*). Indeed, in the case of interesting surface structures involving multiple coordination of adsorbate molecules to a site, the infrared method is probably the most useful method at present for this work, since the observation of characteristic stretching frequencies often leads to an assignment of surface structures.

In this paper we employ an infrared cell designed for working at cryogenic sample temperatures and at higher adsorbate pressures. It has been possible to observe a new adsorption state of CO on Rh^I at high CO pressure which forms as $Rh^I(CO)_2$ is depleted. The infrared spectra were obtained by the multiple-scan data acquisition method making possible the observation of reproducible small changes in band intensity and/or the development of new bands under good signal-to-noise and resolution conditions. Special provisions have been made to eliminate the effect of infrared absorption by the high pressures of CO(g) used.

This paper is divided into two basic parts. In the first part we thoroughly reinvestigate the details of CO adsorption on Rh^I sites to form $Rh^I(CO)_2$ species. The Rh^I surface is prepared by preoxidation of Rh_x^0 sites with O_2 at 309 K. In the second part, building on the earlier results, we perturb the surface reversibly to form small amounts of $Rh^I(CO)_3$ and study this process by ir difference spectroscopy.

II. EXPERIMENTAL

A ratio-recording infrared spectrometer (Perkin–Elmer Model 580B, double beam) equipped with fully computerized data treatment was used for these measurements. For all spectra reported, a 16-scan data accumulation was carried out at resolution = 2.3 or 3.0 cm^{-1}. [Noise-to-signal $\cong$ 5% for signals of the order of 0.05 absorbance unit (A); accumulated scanning time = 2 sec/cm^{-1}]. All spectra in this work have been treated with a 19-point smoothing function. In order to observe small changes in band intensity, subtraction procedures were often used to obtain difference spectra between spectra measured under different conditions. With the advantage of the "half-plate" design shown in Fig. 1, we can properly eliminate the background effects

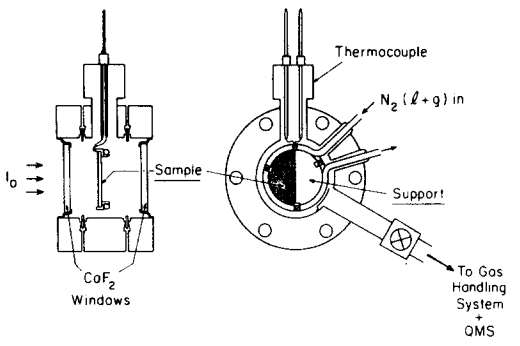

FIG. 1. Ultrahigh vacuum cell for infrared spectroscopy of adsorbed species.

(spectra of CO gas) by making spectroscopic measurements on the Rh/Al_2O_3 half of the sample plate followed by measurements on the Al_2O_3 half plate. Subtraction of the two spectra completely eliminates any effect due to the gas phase. This measurement procedure permits us to work at high CO gas pressures. In the event that an adsorption process occurs on the Al_2O_3, the "half-plate" method also permits this process to be studied independently in detail.

The preparation of the Rh/Al_2O_3 sample has been described previously (*10*). Briefly, suspensions of Rh-free Al_2O_3 and $Rh^{III}Cl_3$–Al_2O_3 mixtures were sprayed on to each half of the CaF_2 plate, respectively. The CaF_2 optical plate was maintained at 350 K to rapidly flash evaporate solvents during the spray deposition. The sample plate was placed in the ir cell and outgassed under vacuum. Following reduction at 423 K in H_2(g), and evacuation of the cell, the sample was placed in the infrared spectrometer. A translation cell holder was used to obtain spectral data on each half of the "half plate."

The CaF_2 plate plus sample is mounted in a copper ring within the cell body which is shown in Fig. 1. This arrangement affords the establishment of any constant temperature between 80 and 310 K by adjusting the flow rate for 1-N_2 coolant. The final "density" of Rh on the Al_2O_3 support was 0.26 $\times$ 10^{-3} g/cm^2 at the 2.2 wt% loading employed here. Total "density" (Rh + Al_2O_3) ranged from 9.9 $\times$ 10^{-3} to 14.4 $\times$ 10^{-3} g/cm^2. The Al_2O_3 "density" on the control side of the sample plate was typically 9.4 $\times$ 10^{-3} g/cm^2. The reduced and preoxidized Rh sample was prepared and studied in the ultrahigh-vacuum stainless-steel infrared cell having CaF_2 windows. The cell was connected to a grease-free bakeable stainless-steel ultrahigh-vacuum system described previously (*10–15*).

Since this study is concerned with the spectroscopic characterization of Rh^I sites containing CO ligands, we chose to eliminate the influence of Rh_x^0 sites by preoxidizing the sample prior to CO adsorption. For this purpose, pure O_2 gas (P_{O_2} = 103 Torr) was admitted for ~5 min to react with the reduced sample surface at 309 K. Very little detectable linear CO or bridged CO (on Rh crystallite sites) were found by infrared studies of the preoxidized Rh surface subjected to CO adsorption. We believe that $Rh^I(CO)_2$ is the major surface species in this work when CO adsorption takes place at low CO pressures on this surface.

The tricarbonyl, $Rh^I(CO)_3$, cannot be observed at room temperature by the infrared method. It has in fact been clear that the condition of low temperature and/or high pressure of CO gas is necessary to achieve a significant population of $Rh^I(CO)_3$ species at the expense of $Rh^I(CO)_2$. All effects reported here for the dicarbonyl/tricarbonyl process are reversible as either P_{CO} or T are changed.

III. RESULTS

A. Activated Production of $Rh^I(CO)_2$—Studies of the Chemisorption Process at Low Temperatures

In a previous paper (*11*), we reported that on Rh/Al_2O_3 surfaces, the *gem*-dicarbonyl species forms extensively via an activated process only above ~180 K when CO(g) is adsorbed on the *reduced samples*. In this work, we have reinvestigated the activated *gem*-dicarbonyl formation on our *oxidized* Rh/Al_2O_3 surface in order to deter-

mine whether the effects reported previously could have involved hypothetical processes such as $Rh_x^0 + CO(g) \xrightarrow{E_a} Rh^I(CO)_2$ where the presence of CO is necessary to promote a surface oxidation process involving other surface species such as surface hydroxyl groups on Al_2O_3 (*31*). As will be shown, it appears that the *gem*-dicarbonyl adsorption process observed on *oxidized* Rh/Al_2O_3 surfaces is very similar to that observed on Rh_x^0 metal clusters.

We begin in Fig. 2A at spectrum (a), where the Rh^I/Al_2O_3 surface is exposed to 0.8 Torr CO pressure at 90 K. Three main ir bands are seen at 2160, 2100, and 2032 cm^{-1}. In addition, there seems to be a broad underlying feature in the 2100-cm^{-1} region which may be a monocarbonyl species $Rh^I(CO)$ (*22*). Reducing the gas-phase pressure to zero by pumping, causes complete loss of the 2160-cm^{-1} band as well as a loss or a loss-plus-shift to lower wavenumber of the broad feature near 2100 cm^{-1} [compare spectrum (b) to spectrum (a)]. The 2160-cm^{-1} band is due to physisorbed CO on Al_2O_3 which is desorbed at 90 K under vacuum.

Subsequent warming of the Rh^I/Al_2O_3 *in vacuo* results in little change in the chemisorbed CO spectra until ~250 K where some decrease in the intensity of the dicarbonyl doublet occurs due probably to desorption in the range 250–309 K (spectra (l) and (m)). It should be noted that the infrared intensities of the features observed in Figs. 2A and B are small compared to those observed for full development of the 2100- and 2032-cm^{-1} bands, as will be seen.

The Rh^I/Al_2O_3 sample was cooled back to 90 K *in vacuo*, and 8.9 Torr of CO(g) was added, giving spectrum (a) in Fig. 3A. At this CO pressure, the surface coverage of physisorbed CO (on Al_2O_3) is higher than in the previous measurement made at 0.8 Torr CO pressure, and features at 2100 and 2032 cm^{-1} are also seen as before. Under CO(g) pressure = 8.9 Torr, the sample was gradually warmed while monitoring the spectral changes [Figs. 3A and B]. It is seen that

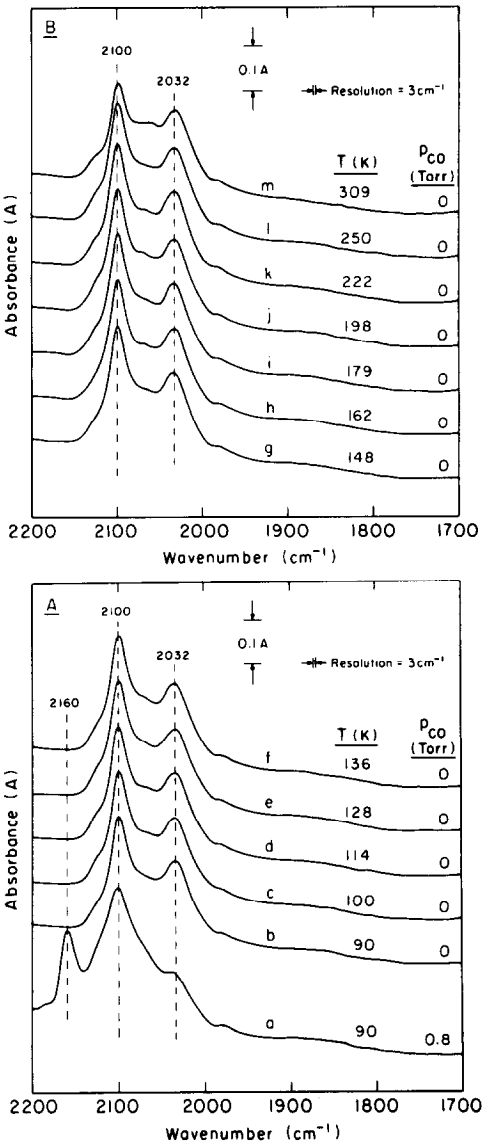

FIG. 2. Infrared spectra for CO adsorption on Rh/Al_2O_3 at 90 K followed by heating under vacuum.

physisorbed CO (2160 cm^{-1}) desorbs first and is gone by about 200 K at 8.9 Torr CO pressure. Near 200 K, both components of the doublet (2100 and 2032 cm^{-1}) begin to intensify strongly and at 309 K, an intensification of the doublet features by about a factor of 5 has taken place.

It is clear by comparison of these results under CO(g) pressure (Figs. 3 and 4) with those obtained under vacuum (Fig. 2) that

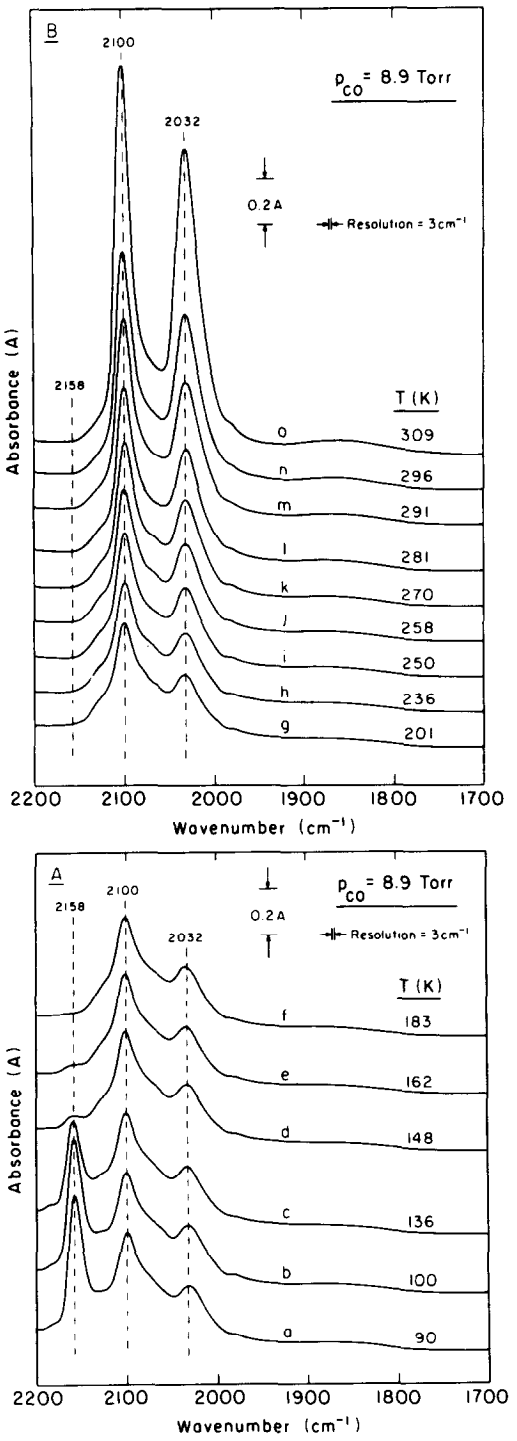

FIG. 3. Activated process producing Rh^{I}(CO)$_2$. (A) At 90–183 K; (B) 201–309 K.

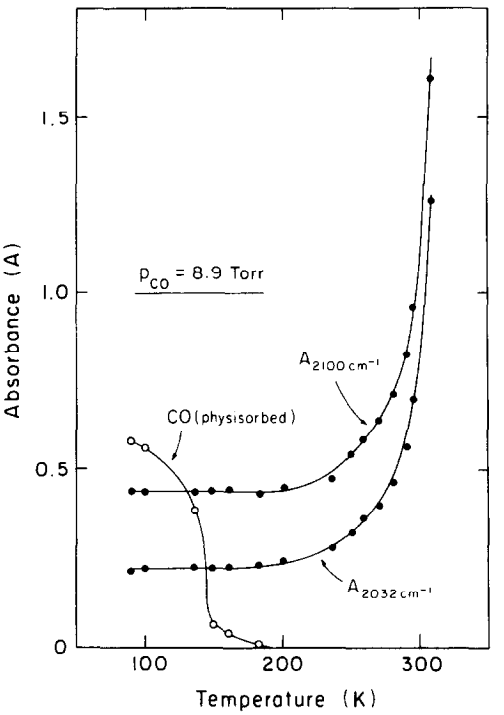

FIG. 4. Temperature dependence of absorbance for CO adsorption on Rh/Al_2O_3.

the activated process to produce Rh^{I}(CO)$_2$ takes place only in the presence of CO(g) and that most of the effect occurs above 200 K. These results are therefore entirely consistent with results obtained previously (*11*) on *reduced* Rh^0_x/Al_2O_3 surfaces, suggesting that the oxygen added to this sample is not involved in this activated process.

The intensity behavior as a function of temperature for the physisorbed and the *gem*-dicarbonyl species is shown in Fig. 4, where it is evident that the activated production of Rh^{I}(CO)$_2$ begins near 200 K.

A plausible explanation for the activated production of Rh^{I}(CO)$_2$ species comes from the recent EXAFS work of Van't Bilk, *et al.* (*34*) who have shown that CO adsorption on small Rh crystallites causes major disruption of the Rh–Rh distances, i.e., the production of isolated sites capable of forming the *gem*-dicarbonyl species. This process could very well be the activated process observed here on oxidized Rh and

previously on reduced Rh_x^0/Al_2O_3 preparations (*11*).

It is also possible that this activated production of $Rh^I(CO)_2$ could be caused by the activated diffusion of CO over the Al_2O_3 support to the Rh^I sites. For a CO diffusion activation energy of 1 kcal mole^{-1} (ΔH_{vap} CO(l) = 1.4 kcal mole^{-1}), at 200 K diffusion distances of the order of 10^{-1} cm in 100 sec would be expected. At 100 K, diffusion over distances of the order of 2×10^{-2} cm in 100 sec would be expected. These distances are of the order of the sample thickness, suggesting that the activated process seen in Fig. 4 is probably not due to CO stratification in our samples.

It should be noted that the fivefold intensification of the $Rh^I(CO)_2$ doublet [2100 and 2032 cm^{-1}] occurs at *constant wavenumber*. This suggests that the Rh^I sites are *isolated* spatially from each other, since close proximity of species should result in oscillator coupling, leading to an increase in wavenumber as surface coverage increases—a well-known effect on single crystal surfaces (*32*).

B. Detailed Study of the gem-Dicarbonyl Infrared Bands at Low CO Coverage

The data of Fig. 3 indicate that there is essentially no shift of the 2 bands associated with $Rh^I(CO)_2$ over a wide range of surface coverage up to saturation. In order to be certain that "inhomogeneous broadening" is not present for these features, a second approach was employed. We have studied CO adsorption on a second Rh^I/Al_2O_3 sample, starting from the lowest CO coverages possible and carefully examining spectral developments as coverage is increased. These experiments were carried out at 309 K as shown in Fig. 5. Spectrum (a) is our background spectrum and it exhibits small features of about 0.01 *A* units in intensity. These features are probably due to CO adsorption on the surface from the background CO present in the vacuum apparatus. Small quantities of CO(g) are added in successive experiments, and it

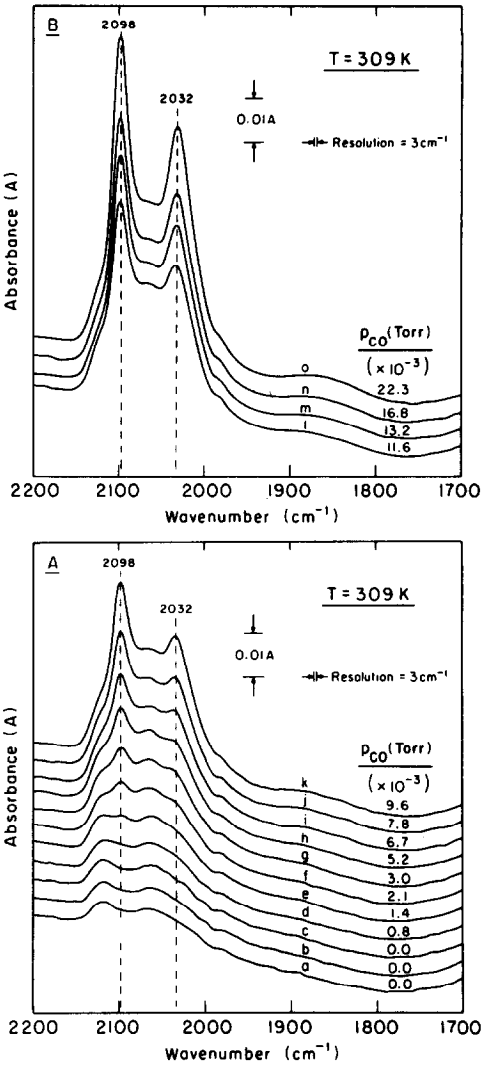

FIG. 5. Development of ir spectra for low coverage CO on Rh/Al_2O_3. (A) First adsorption stage; (B) second adsorption stage.

may be seen that the *gem*-dicarbonyl peaks begin to grow at 2098 and 2032 cm^{-1}. Figure 5A shows 11 spectra taken sequentially; the sequence is continued in Fig. 5B. No observable shift is observed as the spectral features intensify in this low coverage range.

In order to more thoroughly examine the spectral behavior in this low coverage range, difference spectra were calculated using every other spectrum in Figs. 5A and B. The sequence of difference spectra are

shown in Fig. 6, where, by the subtraction process, the development of the dicarbonyl doublet features is enhanced in comparison to the weaker and broader underlying features present in the original spectra in Figs. 5A and B. Once again, there appears to be no systematic shift of the *gem*-dicarbonyl features for incremental changes in CO coverage. Furthermore, all of the difference spectra are positive spectra over their entire wavenumber range, indicating that we are observing a *filling* of adsorption sites rather than any kind of coverage dependent species *conversion* process which would result in depletion of a species, leading possibly to negative-going features in the difference spectra.

Previous general considerations have led to the assignment of the 2098-cm^{-1} feature as the symmetrical stretching mode for Rh^I(CO)$_2$, and the 2032-cm^{-1} feature as the asymmetrical stretching mode (*33*). If a single species is being produced, the ratio of peak intensity of these two modes should be invarient with CO coverage. Figure 7 shows that this is true in the low coverage range of data represented in Figs. 5A and B, to within the accuracy possible in the presence of smaller interfering absorption bands mentioned previously.

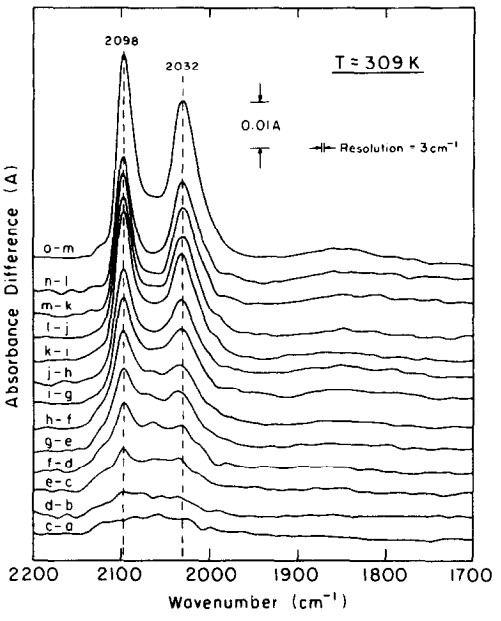

FIG. 6. Sequence of difference spectra during the development of Rh^I(CO)$_2$ species at low CO coverage.

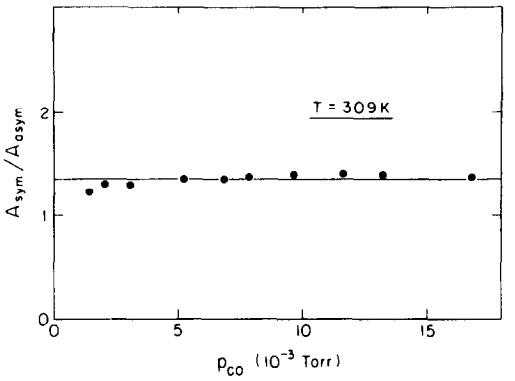

FIG. 7. Peak absorbance ratio of the Rh^I(CO)$_2$ doublet during chemisorption for low coverage CO on Rh/Al_2O_3.

Thus, we conclude that the behavior of the *gem*-dicarbonyl spectra are as expected for an array of *isolated* adsorption sites. The constancy in wavenumber and in peak absorbance ratio over the initial coverage range suggests that the *isolated* Rh^I sites are also *chemically similar*, and that the width of the ir bands may be most appropriately considered to be due to *homogeneous broadening effects* associated with the chemically similar surface species. In other words, there is only one kind of Rh^I surface site supported on the Al_2O_3 substrate as judged by the chemical similarity of the Rh^I(CO)$_2$ species produced over a wide coverage range.

C. *Detection of Rh^I(CO)$_3$ at High CO Pressure*

Figure 8A shows two infrared spectra obtained for the Rh^I/Al_2O_3 substrate under high CO pressures at 241 K. The dotted line is the spectrum under 62 Torr CO pressure, while the solid line is the spectrum at 423 Torr CO pressure. Each spectrum is the difference measured between the Rh/Al_2O_3 half and the Al_2O_3 half plate. Thus, since the optical path length and the gas tempera-

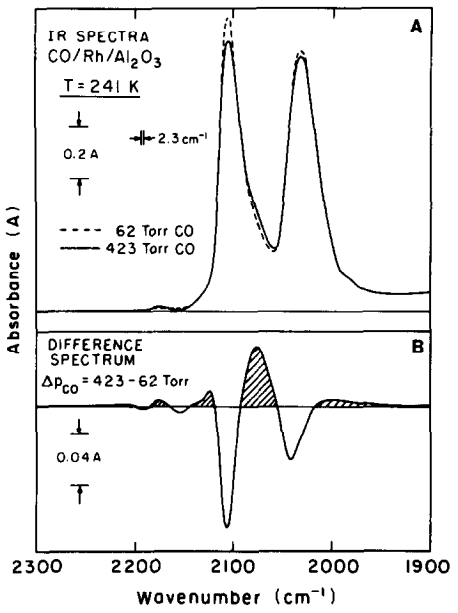

FIG. 8. (A) Infrared spectra of high coverage CO on Rh/Al_2O_3. The dotted line is the spectrum under 62 Torr CO pressure, while the solid line is the spectrum at 423 Torr pressure. (B) Difference spectrum.

ture are identical for the two measurements, the spectra as shown in Fig. 8A do not contain any contribution from the high pressure gas phase CO.

The most notable differences observed in the two spectra are an intensity *decrease* in *both gem*-dicarbonyl features as P_{CO} is raised at constant temperature. In addition, a small *increase* in intensity is noted in the spectral region between the two sharp bands as P_{CO} is increased. There are also other small effects at wavenumbers above and below the *gem*-carbonyl peaks. These small differences are quite *reproducible* and *reversible*. They are most easily seen by taking difference spectra as shown in Fig. 8B.

Figure 9 shows six ir spectra measured between 62 and 423 Torr CO pressure at a constant temperature of 241 K. The systematic behavior which occurs in intensity is most easily seen by plotting difference spectra between the 62-Torr condition and the higher P_{CO} conditions. By comparison of the sequential difference spectra it can be seen that *very systematic changes occur* in the range 2200–1950 cm^{-1} as the CO pressure is increased (Fig. 10).

The most dramatic effects seen in these difference spectra are the monotonic *decrease* in the intensity of the *gem*-dicarbonyl peaks coupled systematically with an increase of a new feature centered near 2077 cm^{-1}. In addition, smaller positive features are seen at 2120 and 2180 cm^{-1}, as well as a broad positive feature near 1990 cm^{-1}. Small *negative* features develop monotonically with CO pressure increase at 2155 and 2190 cm^{-1}.

It is important to note the fact that as P_{CO} is increased, the 2032-cm^{-1} asymmetric stretching mode for $Rh^I(CO)_2$ does not decrease in absolute peak intensity as rapidly as the 2105-cm^{-1} symmetric stretching mode (see Fig. 11).

This large difference in differential intensity behavior of the 2032-cm^{-1} mode compared to the 2105-cm^{-1} mode is inconsistent with expectations for the $Rh^I(CO)_2$ species

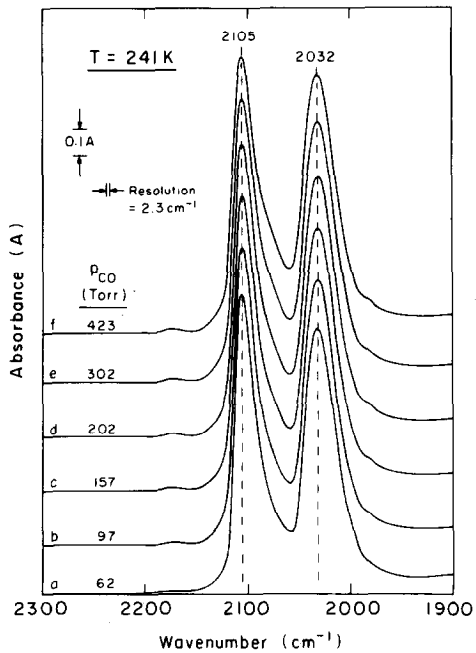

FIG. 9. Development of ir spectra for high coverage CO on Rh/Al_2O_3.

and is also inconsistent with the experimental result of Fig. 7, where an invariant ratio of peak intensities has been measured. The observed difference in intensity behavior suggests that for high P_{CO}, the 2032-cm^{-1} feature is overlapped significantly by a spectral band which is close to 2032 cm^{-1} in wavenumber, but which grows positively as the 2032-cm^{-1} feature disappears. The hypothesis of an overlapping band is supported by the observation that the negative feature in Fig. 10 is at 2042 cm^{-1}, 10 cm^{-1} above the $Rh^I(CO)_2$ asymmetric stretching mode at 2032 cm^{-1}. The hypothesis is further supported by the observation of an inflection point near 2032 cm^{-1} in the negative difference peaks shown at 2042 cm^{-1} in Fig. 10. It should be noted that in contrast to the 2042-cm^{-1} behavior, the negative peak corresponding to the loss of intensity of the symmetric stretch (2108 cm^{-1}) is only 3 wavenumbers above the peak frequency at 2105 cm^{-1} (Fig. 10 compared to Fig. 9).

The overlap in the difference spectra (Fig. 10) of a postulated positive tricarbonyl band with the negative 2032-cm^{-1} band was

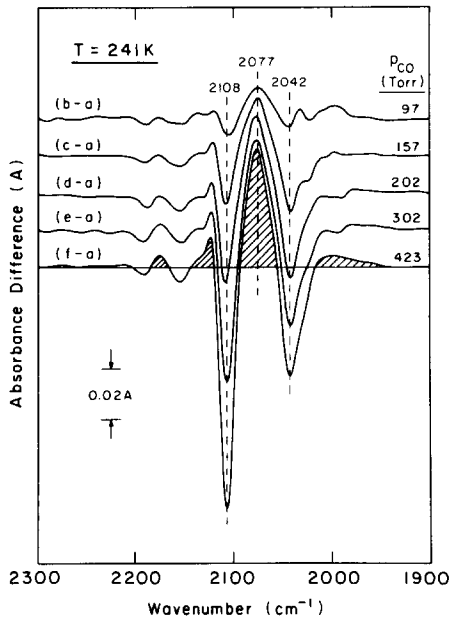

FIG. 10. Sequential difference spectra for high coverage CO on Rh/Al_2O_3.

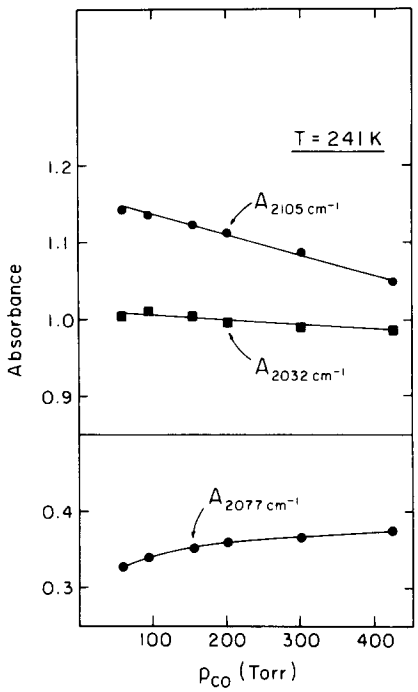

FIG. 11. Peak absorbance changes for high coverage CO on Rh/Al_2O_3.

further investigated as follows. The fully ^{12}CO-covered surface was cooled to 90 K under vacuum and exposed to $^{13}CO(g)$ (99%) at 1.2 Torr. If the process $Rh^I(^{12}CO)_2 + {}^{13}CO(g) \rightarrow Rh^I(^{12}CO)_2(^{13}CO)$ occurs, the carbonyl stretching frequencies of the partially labeled tricarbonyl species will be at lower wavenumbers than in the unlabeled case. If there is an overlap of a $Rh^I(^{12}CO)_2$ band at 2032 cm^{-1} with a tricarbonyl band, this overlap will be reduced or eliminated for the labeled tricarbonyl. Thus one would predict that the negative difference peak seen at 2042 cm^{-1} in Fig. 10 should become even more negative and should move closer to 2032 cm^{-1} when the interference is removed. Also, one would predict that a positive difference feature should be more pronounced below 2000 cm^{-1} due to the separation of the overlap by the process of isotopic substitution. Both of these predictions are verified by experiment as shown in Fig. 12. A strongly enhanced symmetric

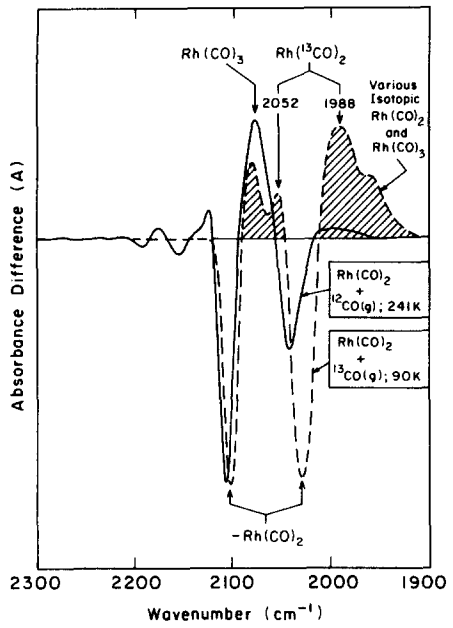

FIG. 12. Comparison of (difference spectra) for $Rh^I(CO)_2$ + ^{12}CO(g) at 241 K and $Rh^I(CO)_2$ + ^{13}CO(g) at 90 K.

stretch difference peak (more negative) is observed at 2030 cm^{-1}, and strongly enhanced positive features below 2000 cm^{-1} are also observed. The calculated positions of $Rh(^{13}CO)_2$ features are shown at 2052 and 1988 cm^{-1}, and contributions from this exchanged species may be present also. Thus, at 90 K, both $Rh^I(CO)_2$ and $Rh^I(CO)_3$ and various combinations of exchanged $Rh^I(CO)_2$ and $Rh^I(CO)_3$ are likely to be present, making detailed spectral deconvolution impossible in this case.

D. Detection of $Rh^I(CO)_3$ at High Pressures of CO and at Low Temperatures

If a weakly bonded $Rh^I(CO)_3$ is able to be produced from $Rh^I(CO)_2$ by raising P_{CO}, it is also likely that lowering the substrate temperature in excess CO will achieve the same basic result. This possibility has been explored, and difference spectra are compared (Fig. 13) at various temperatures with the 263 K/65 Torr baseline spectrum.

It is immediately evident that the phenomenon observed on *raising* P_{CO} at constant temperature is also occurring at constant P_{CO} *as the temperature is lowered.* Strong negative peaks are observed at a wavenumber limit of 2108 and 2038 cm^{-1} (systematically shifted from lower wavenumbers as the temperature is reduced). In addition, in Fig. 13, a trio of positive features reminiscent of those found in the CO pressure change experiments (Fig. 10) are observed to increase monotonically as the temperature is reduced. The observed negative difference peak due to physisorbed CO (2160 cm^{-1}) is probably related to the fact that excess Al_2O_3 surface area is present on the Al_2O_3-half of the sample plate, and subtraction of this spectrum leads to a negative effect in the difference.

While the results seen in Fig. 13 are qualitatively similar to those obtained by increasing P_{CO} at constant temperature (Fig. 10), there are differences in detail due primarily to the fact that the wavenumber of the $Rh^I(CO)_2$ vibrational modes will shift to higher values by 2–3 cm^{-1} over the temperature range studied here. This effect of tem-

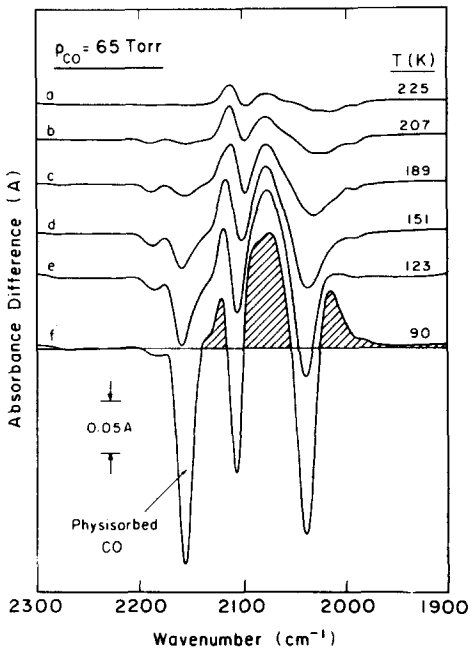

FIG. 13. Difference spectra for CO on Rh/Al_2O_3 upon cooling in CO(g).

perature has been well studied (*35*) and will not be discussed further.

IV. DISCUSSION

A. *Deconvolution of the ir Spectrum of $Rh^I(CO)_3$*

We have attempted to analyze the data presented in Fig. 9 using additional criteria for subtraction of spectra. Assume that as the process $Rh^I(CO)_2 + CO(g) \rightarrow Rh^I(CO)_3$ occurs with increasing P_{CO}, the fraction $F_{Rh^I(CO)_2}$ of $Rh^I(CO)_2$ is consumed by conversion to $Rh^I(CO)_3$. Thus, at a given P_{CO}, the $Rh^I(CO)_2$ spectrum should be attenuated by the factor $(1 - F_{Rh^I(CO)_2})$ in comparison to that existing at a lower P_{CO}. If we assume that the best estimate of $F_{Rh^I(CO)_2}$ can be made on the basis of absorbance measurements at 2105 cm^{-1} (the symmetric CO stretch peak at these high coverages), then the factor $(1 - F_{Rh^I(CO)_2})$ can be determined. This was done at 241 K for P_{CO} values ranging from 97 up to 423 Torr, and the attenuation factor was applied to the 65 Torr/241 K base spectrum. By subtracting the *attenuated* base spectrum at 65 Torr from the measured spectra at higher P_{CO} values, a set of difference spectra are produced which should approximately represent the spectrum of $Rh^I(CO)_3$. These data are shown in Fig. 14 over the range of P_{CO} from 97 to 423 Torr. Three major positive absorbance features are seen at 2120, 2078, and 2026 cm^{-1}. The absorbance of these three features increases monotonically (and at essentially constant wavenumbers) as P_{CO} is increased, although intensity ratios vary slightly over the range of the experiment.

We have employed other more arbitrary criteria for determining $F_{Rh^I(CO)_2}$ in order to attempt to deconvolute the $Rh^I(CO)_3$ spectrum from the stronger $Rh^I(CO)_2$ spectrum. The other methods give slightly different band shapes and peak positions, but, *in all cases, three peaks are found for the $Rh^I(CO)_3$ species, having wavenumbers near those shown in Fig. 14.*

In Fig. 14, the fact that consistent spectra

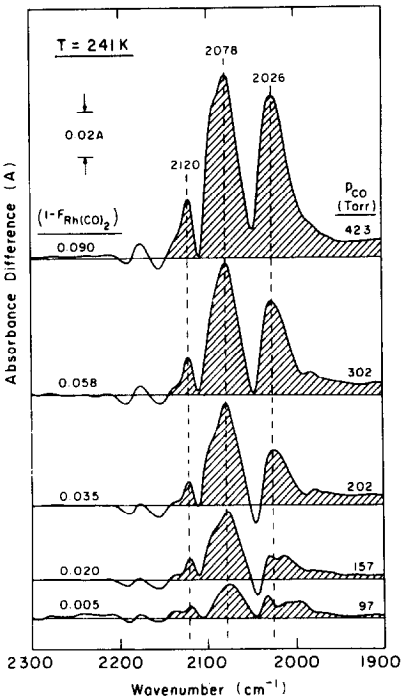

FIG. 14. Deconvoluted ir spectra of $Rh^I(CO)_3$ on Rh/Al_2O_3.

for $Rh^I(CO)_3$ develop together (in a reversible fashion) suggests that all three peaks are associated with the same species, although one cannot completely eliminate the possibility that one of the peaks may be associated with another kind of Rh site on these surfaces. Indeed, the small positive and negative difference peaks above 2150 cm^{-1} are probably associated with minor carbonyl species for Rh sites of oxidation numbers II or III.

Rice *et al.* (*25*) have reported the existence of a carbonyl band at 2120 cm^{-1} which is present only on *oxidized* Rh/Al_2O_3 surfaces. This is assigned to a $Rh^{II}(O)(CO)$ species and it forms at *low CO pressures* on the oxidized surface. We see this feature also (Figs. 5 and 6) at low CO pressures on the oxidized Rh/Al_2O_3 surface. However, the reversible 2120-cm^{-1} feature observed in the difference spectra of Fig. 10, and also in Fig. 14 is thought to be due to another species, and is assigned in this work as a band due to $Rh^I(CO)_3$.

B. *Interpretation of the Spectrum for* $Rh^I(CO)_3$

For both $Rh^I(CO)_2$ (C_{2v}) and $Rh^I(CO)_3$ (C_{3v}) one expects to observe two ir bands due to symmetric and asymmetric coupling of the carbonyl groups (*36*). However, in the case of a Rh^I site which may be held on a multicoordinated site on the Al_2O_3 surface, the symmetry rules applying to C_{2v} or C_{3v} symmetry groups may be relaxed and additional infrared active modes are permitted. This reduction to lower symmetry can be thought of as a local interaction effect, making one of the three carbonyl ligands inequivalent to the other two, resulting in a splitting of the lower frequency band (E mode) (*37*). Examples are known where metal tricarbonyls, experiencing anisotropy in solvation, show slight splitting of the E mode. In addition, unsymmetrical bonding of additional ligands to the metal center of tricarbonyls can lead to three carbonyl stretching modes, and many examples are given in Table 7.14 of Ref. (*37*).

We believe that the bonding of the Rh^I site to the Al_2O_3 surface is likely to occur at a multicoordinated site which leads to the observed three-band spectrum for $Rh^I(CO)_3$. Bonding of analogous species [$Mo(CO)_3$] to Al_2O_3 in various stages of dehydroxylation produces a species exhibiting three carbonyl stretching modes, and tentative site assignments on the Al_2O_3 have been made (*38*). A good analogy to our proposed $Rh^I(CO)_3$ species [2120, 2078, and 2026 cm^{-1}] may be $Mn(CO)_3(dppe)^I$ Br^+ [2104, 2069, and 2016 cm^{-1}] (*37*), as shown in Fig. 15.

In addition, Morris and Tinker (*39*), using a high-pressure ir cell *at 298 K*, were able to convert dissolved $[Rh^I(CO)_2X]_2$ to $Rh^I(CO)_3X$ at 13–33 atm CO pressure. The efficiency of the reversible conversion depended on solvent composition and on the identity of X = Cl, Br, I, ranging from 8 to 100% conversion. The $Rh^I(CO)_3X$ species displayed a carbonyl doublet at about 2100

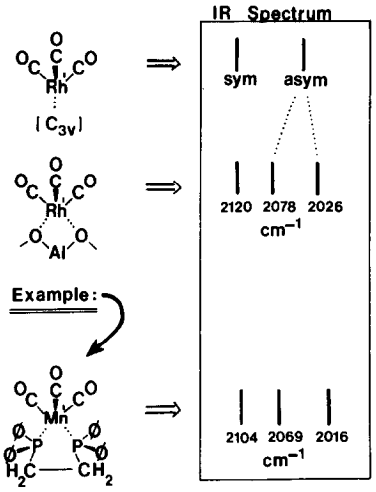

FIG. 15. Possible structure of $Rh^I(CO)_3$ on Al_2O_3 and comparison of ir spectra.

and 2050 cm^{-1}, consistent with C_{3v} symmetry. These results are therefore quite consistent with our findings for alumina-supported $Rh^I(CO)_2$ conversion to $Rh^I(CO)_3$.

It is sometimes noted that tricarbonyl species exhibit lower ir intensity in the high frequency mode compared to the other modes. Examples of this behavior may be found for L–$Fe(CO)_3$ and L–$Fe(X)(CO)_3$ species where L = olefinic or allylic ligand and X = Cl or Br (*40*). In addition, low symmetry L_3–$M(CO)_3$ species invariably yield a high-frequency carbonyl mode of low intensity (*41*).

Thus, on the basis of the presence of three observed carbonyl bands, the analogy of band frequencies to compounds of known stoichiometry and structure, the observed intensity ratios, and the methods of preparation, we assign the difference spectrum in Fig. 14 to $Rh^I(CO)_3$ bound in an unsymmetric Al_2O_3 bonding site. We cannot completely eliminate the possibility that we are observing two species whose thermodynamics are so similar that parallel intensity behavior occurs on raising P_{CO} or lowering the temperature, giving the essentially similar results shown in Figs. 10 and 13. This coincidence is unlikely however.

[1] Where dppe stands for $Ph_2PC_2H_4P\,Ph_2$.

V. SUMMARY OF RESULTS

The following conclusions have been reached on the basis of this work, carried out on Rh^I/Al_2O_3 surfaces produced by oxidation of supported Rh/Al_2O_3 preparations.

(1) $Rh^I(CO)_2$ formation occurs via an activated process in which CO(g) is an essential participant in the activated step. The onset of the process is near 200 K.

(2) The carbonyl stretching modes for $Rh^I(CO)_2$ occur near 2098 and 2032 cm^{-1}, and there is no evidence for a mixture of different types of Rh^I sites on Al_2O_3.

(3) The reversible reaction $Rh^I(CO)_2 + CO(g) \rightarrow Rh^I(CO)_3$ occurs at higher P_{CO} and lower T. It is likely that the facile isotopic exchange into $Rh^I(CO)_2$ takes place via the formation of more weakly bound CO ligands in the $Rh^I(CO)_3$ species.

(4) The infrared spectrum of $Rh^I(CO)_3/Al_2O_3$ exhibits three carbonyl stretching modes at about 2120, 2078, and 2026 cm^{-1}. This indicates that the Rh^I center is multicoordinately bound to Al_2O_3, lowering the symmetry of $Rh^I(CO)_3$ below C_{3v}.

(5) The results shown here illustrate the capability of high-sensitivity ir difference spectroscopy for studying minority surface species which can only be populated at low temperatures and/or high gas pressures.

ACKNOWLEDGMENTS

The authors acknowledge the support of this work by a research grant from the Science Research Laboratory and the 3M Central Research Laboratories, St. Paul, Minnesota. We also acknowledge stimulating discussions with Dr. Allen Siedle of 3M and with Professor Graham Mott of the University of Pittsburgh.

REFERENCES

1. Yates, D. J. C., Murrell, L. L., and Prestridge, E. B., *J. Catal.* **57,** 41 (1979).
2. Katzer, J. R., Sleigh, A. W., Gajardo, P., Michel, J. B., Gleason, E. F., and McMillan, S., *Faraday Discuss.* **72,** 121 (1981).
3. Knozinger, H., Thornton, E. W., and Wolfe, M., *J. Chem. Soc. Faraday I* **75,** 1898 (1979).
4. Theshir, A., Smith, A. K., Lecomte, M. S., Basset, J. M., Zonderighi, G. M., Psaro, R., and Ugo, R., *J. Organomet. Chem.* **191,** 415 (1980).
5. Bilhou, J. L., Bilhou-Bougnol, V., Graydon, W. F., Basset, J. M., Smith, A. K., Zonderighi, G. M., and Ugo, R., *J. Organomet. Chem.* **153,** 73 (1978).
6. Primet, M., Vidrine, J. C., and Nacchache, C., *J. Mol. Catal.* **4,** 411 (1978).
7. Rice, C. A., Worley, S. D., Curtis, C. W., Guin, J. A., Tarrer, A. R., *J. Chem. Phys.* **74,** 6487 (1981).
8. Conesa, J. C., Sainz, M. T., Soria, J., Munuera, G., Rives-Arnau, V., and Muñoz, A., *J. Mol. Catal.* **17,** 231 (1982).
9. Foley, H. C., DeCanio, S. J., Tan, K. D., Charu, K. C., Onsferko, J. H., Dybowski, C., and Gates, B. C., *J. Amer. Chem. Soc.* **105,** 3074 (1983).
10. Yates, J. T., Jr., Duncan, T. M., Worley, S. D., and Vaughan, R. W., *J. Chem. Phys.* **70,** 1219 (1979).
11. Yates, J. T., Jr., Duncan, T. M., and Vaughan, R. W., *J. Chem. Phys.* **71,** 3908 (1979).
12. Cavanagh, R. R., and Yates, J. T., Jr., *J. Chem. Phys.* **74,** 4150 (1981).
13. Antoniewicz, P. R., Cavanagh, R. R., and Yates, J. T., Jr., *J. Chem. Phys.* **73,** 3456 (1980).
14. Cavanagh, R. R., and Yates, J. T., Jr., *J. Catal.* **68,** 22 (1981).
15. Yates, J. T., Jr., and Kolasinski, K., *J. Chem. Phys.* **79,** 1026 (1983).
16. Yang, A. C., and Garland, C. W., *J. Phys. Chem.* **61,** 1504 (1957).
17. Yates, J. T., Jr., Duncan, T. M., Worley, S. D., and Vaughan, R. W., *J. Chem. Phys.* **70,** 1219 (1979).
18. Yates, J. T., Jr., Worley, S. D., Duncan, T. M., and Vaughan, R. W., *J. Chem. Phys.* **70,** 1225 (1979).
19. Duncan, T. M., Yates, J. T., Jr., and Vaughan, R. W., *J. Chem. Phys.* **73,** 975 (1980).
20. Yates, J. T., Jr., and Cavanagh, R. R., "Proceedings, 4th International Conference on Solid Surfaces," Supplement a la Revue, Le Vide (Journal of French Vacuum Society), p. 750. (1980).
21. Iizuka, T., and Lunsford, J., *J. Mol. Catal.* **8,** 391 (1980).
22. Primet, M., *J. Chem. Soc. Faraday Trans. I* **74,** 2570 (1978).
23. Knozinger, H., Thornton, E. W., and Wolf, M., *J. Chem. Soc. Faraday Trans. I* **75,** 1888 (1979).
24. Yates, D. J. C., Murrell, L. L., and Prestridge, E. B., *J. Catal.* **57,** 41 (1979).
25. Rice, C. A., Worley, S. D., Curtis, C. W., Guin, J. A., and Tarrer, A. R., *J. Chem. Phys.* **74,** 6487 (1981).
26. Worley, S. D., Rice, C. A., Mattson, G. A., Curtis, C. W., Guin, J. A., and Tarrer, A. R., *J. Phys. Chem.* **86,** 2714 (1982).
27. Yates, J. T., Jr., and Kolasinski, K., *J. Chem. Phys.* **79,** 1026 (1983).
28. Yates, J. T., Jr., and Goodman, D. W., *J. Chem. Phys.* **73,** 5371 (1980).

29. Little, L. H., "Infrared Spectra of Adsorbed Species." Academic Press, New York/London, 1966.
30. Hair, M. L., "Infrared Spectroscopy in Surface Chemistry." Dekker, New York, 1967.
31. Bowman, R. G., and Burwell, R. L., *J. Catal.* **63,** 463 (1980).
32. Bradshaw, A., *Appl. Surf. Sci.* **11/12,** 712 (1982).
33. Cotton, F. A., and Wilkinson, G., "Advanced Inorganic Chemistry," 3rd ed., p. 701. Wiley, New York, 1972.
34. Van't Bilk, H. F. A., Dvon Zon, J. B. A., Hulzinga, T., Vis, J. C., Koningsberger, D. C., and Prins, R., *J. Phys. Chem.* **87,** 2264 (1983).
35. Antoniewicz, P. R., Cavanagh, R. R., and Yates, J. T., Jr., *J. Chem. Phys.* **73,** 3456 (1980).
36. Nakamoto, K., "Infrared and Raman Spectra of Inorganic and Coordination Compounds," 3rd ed., p. 293. Wiley, New York, 1978.
37. Braterman, P. S., "Metal Carbonyl Spectra," 1st ed., p. 46. Academic Press, New York/London, 1975.
38. Laniecki, M., and Burwell, R. L., *J. Colloid Interface Sci.* **75,** 95 (1980).
39. Morris, D. E., and Tinker, H. B., *J. Organometal Chem.* **49,** C53–56 (1973).
40. Noack, K., *Helv. Chim. Acta* **45,** 1847 (1962).
41. Ash, M. J., Brookes, A., Knox, S. A. R., and Stone, F. G. A., *J. Chem. Soc. (A)*, 458 (1971).